Multifractional Brownian Motion with Telegraphic, Stochastically Varying Exponent

Michał Balcerek[1] Samudrajit Thapa[2,3,*] Krzysztof Burnecki[1] Holger Kantz[2] Ralf Metzler[4] Agnieszka Wyłomańska[1] and Aleksei Chechkin[1,4,5,6]

[1]*Faculty of Pure and Applied Mathematics, Hugo Steinhaus Center, Wrocław University of Science and Technology, Wybrzeże Wyspiańskiego 27, 50-370 Wrocław, Poland*

[2]*Max Planck Institute for the Physics of Complex Systems, Noethnitzer Straße 38, 01187 Dresden, Germany*

[3]*Department of Physics, Indian Institute of Technology Guwahati, Guwahati 781039, Assam, India*

[4]*Institute of Physics & Astronomy, University of Potsdam, 14476 Potsdam, Germany*

[5]*German-Ukrainian Core of Excellence, Max Planck Institute of Microstructure Physics, Weinberg 2, 06120 Halle, Germany*

[6]*Akhiezer Institute for Theoretical Physics, National Science Center "Kharkiv Institute of Physics and Technology," Akademichna str.1, Kharkiv 61108, Ukraine*

(Received 30 October 2024; accepted 10 April 2025; published 12 May 2025)

The diversity of diffusive systems exhibiting long-range correlations characterized by a stochastically varying Hurst exponent calls for a generic multifractional model. We present a simple, analytically tractable model which fills the gap between mathematical formulations of multifractional Brownian motion and empirical studies. In our model, called telegraphic multifractional Brownian motion, the Hurst exponent is modeled by a smoothed telegraph process which results in a stationary beta distribution of exponents as observed in biological experiments. We also provide a methodology to identify our model in experimental data and present concrete examples from biology, climate, and finance to demonstrate the efficacy of our approach.

DOI: 10.1103/PhysRevLett.134.197101

When creating the mathematical basis of the theory of locally homogeneous isotropic turbulence [1], Kolmogorov introduced a new class of random processes called *"Wiener spirals,"* which are Gaussian self-similar processes with stationary, power-law correlated increments [2,3]. The theory of Wiener spirals has received further development in mathematical literature [4–6]; however, the theory remained almost unknown to a broader scientific community until 1968, when Mandelbrot and van Ness [7] presented an explicit integral representation for such process that they called *"fractional Brownian motion"* (FBM). FBM has become a paradigmatic example of a Gaussian random process whose scaling properties are characterized by a unique index H called *Hurst exponent* $(0 < H < 1)$ [8]. It exhibits persistent behavior (i.e., supporting the existing tendency) when $1/2 < H < 1$, and antipersistent behavior (supporting the opposite tendency) when $0 < H < 1/2$. In anomalous diffusion theory the diffusion exponent characterizing the time dependence of the mean squared displacement (MSD) for FBM equals $2H$, thus reflecting either fast (super-), or slow (sub-) diffusion for $H > 1/2$ and $H < 1/2$, respectively [9–12]. The case $H = 1/2$ corresponds to ordinary Brownian motion, or the Wiener process $B(t)$ [9]. Numerous phenomena exhibiting FBM-like behavior were found in diverse fields, from telecommunications, engineering [13,14], and image processing [15] to astrophysics [16], climate [17,18], underground water transport [19], and from movement ecology [20,21], intracellular motion [11,22,23], and paths of nerve fibers [24] to financial mathematics [8,25].

However, both hallmarks of FBM, power-law correlations and self-similarity, imply strong idealizations which often are not realized in practice. As a generalization of FBM, *multifractional Brownian motion* (MBM) was introduced in the mathematical literature: a random process characterized by a function $H(t)$ which can be either deterministic or random [26–33]. Indeed, in many experimental observations there is evidence that the Hurst exponent H randomly varies from realization to realization or even along a single sample path. Such doubly stochastic behavior was observed in financial data [34–36], segmentation of images [37], pollution data [38], and recently in several single-particle tracking (SPT) experiments [39–54]. Therefore, it is likely a generic feature of a certain class of systems. However, to the best of our knowledge, there is an absence of generic analytical models of MBM to compare with the empirical observations.

*Contact author: thapa@pks.mpg.de

In this Letter we aim at filling the gap between mathematical formulations of MBM with random Hurst exponent and experiments by introducing *telegraphic multifractional Brownian motion* (TeMBM), a simple generic analytical model mimicking smooth variations of the Hurst exponent along the sample path. We provide a methodology to distinguish between three classes of power-law correlated random processes, namely FBM (with fixed Hurst exponent), FBM with Hurst exponent varying between different realizations, and TeMBM. We present examples from biology, climate, and finance to demonstrate the efficacy and applicability of our approach.

We define MBM with random Hurst exponent via the spectral representation [27–29,31]

$$B_{\mathcal{H}}(t) = C(\mathcal{H}(t)) \int_{-\infty}^{\infty} \frac{e^{i\omega t} - 1}{|\omega|^{\mathcal{H}(t)+1/2}} dB(\omega), \quad t \geq 0, \quad (1)$$

where $dB(\omega)$ is "the Fourier transform" of the white noise $dB(t)$ with $\langle dB(\omega_1) dB(\omega_2)\rangle = \delta(\omega_1 + \omega_2) d\omega_1 d\omega_2$ [33], and $\mathcal{H}(t)$ is a stationary process which is independent of $B(t)$. Its probability density function (PDF) $p(h)$ is defined on the interval $0 \leq h \leq 1$. The prefactor $C(\mathcal{H}(t)) = \sqrt{\Gamma(2\mathcal{H}(t)+1)\sin(\pi\mathcal{H}(t))}/\sqrt{2\pi}$ is chosen such that the MSD conditional on $\mathcal{H}(t)$ is $\langle (B_{\mathcal{H}}(t) - B_{\mathcal{H}}(0))^2\rangle = t^{2\mathcal{H}(t)}$.

The autocovariance function (ACVF) of $B_{\mathcal{H}(t)}$ conditional on $\mathcal{H}(t)$ thus takes the form

$$\langle B_{\mathcal{H}}(t) B_{\mathcal{H}}(s)\rangle = D(\mathcal{H}(t), \mathcal{H}(s)) \left(t^{\mathcal{H}(t)+\mathcal{H}(s)} + s^{\mathcal{H}(t)+\mathcal{H}(s)}\right) - D(\mathcal{H}(t), \mathcal{H}(s)) |t-s|^{\mathcal{H}(t)+\mathcal{H}(s)}, \quad (2)$$

where the function $D(x, y)$ is defined as (see Sec. I in Supplemental Material [55] for more details)

$$D(x, y) = \frac{\sqrt{\Gamma(2x+1)\Gamma(2y+1)\sin(\pi x)\sin(\pi y)}}{2\Gamma(x+y+1)\sin(\frac{\pi(x+y)}{2})}. \quad (3)$$

Note that if $\mathcal{H}(t)$ is constant, Eq. (2) reduces to the well-known ACVF which uniquely defines the Kolmogorov-Mandelbrot FBM. The PDF of $B_{\mathcal{H}}(t)$ is given by

$$P(x, t) = \frac{1}{\sqrt{2\pi}} \int_{-\infty}^{\infty} \frac{\exp\{-x^2/(2t^{2h})\}}{t^h} p(h) dh, \quad (4)$$

where $p(h)$ is defined below.

To go further we need to specify the process $\mathcal{H}(t)$. Here we propose to model the temporal variability of the Hurst exponent with a stationary smoothed telegraph process defined through the stochastic differential equation

$$\frac{d\mathcal{H}(t)}{dt} = \frac{-\mathcal{H}(t) + \mathcal{H}_{TP}(t)}{\tau}, \quad (5)$$

where τ is the relaxation time and $\mathcal{H}_{TP}(t)$ is a telegraph process, i.e., a stationary dichotomic Markov process that jumps between the two values H_1 and H_2, $0 \leq H_1 < H_2 \leq 1$, with mean rates $\lambda(H_1 \to H_2) = \lambda_{12}$ and $\lambda(H_2 \to H_1) = \lambda_{21}$. We call the resulting process $B_{\mathcal{H}}(t)$ TeMBM. We note that the telegraph process and its extensions are useful to model financial market dynamics [62–65] as well as the dynamics in biological systems, for example, gene expression [66,67] or when myosin motors exert contractile forces on the cytoskeleton network [68–72]. Our proposed choice of $\mathcal{H}(t)$ is advantageous for several reasons. Formally, it results in bounded and smooth variations of the random Hurst exponent. Furthermore, in the stationary state the PDF is given by the beta distribution (see [73] and Sec. II in Supplemental Material [55])

$$p(h) = \frac{(h - H_1)^{\lambda_{12}\tau - 1}(H_2 - h)^{\lambda_{21}\tau - 1}}{(H_2 - H_1)^{2\lambda\tau - 1} B(\lambda_{21}\tau, \lambda_{12}\tau)}, \quad (6)$$

where $H_1 \leq h \leq H_2$, $\lambda = (\lambda_{12} + \lambda_{21})/2$ and $B(x, y)$ is the beta function. As can be seen from Eq. (6), this distribution has four typical shapes (see Fig. 1 in Supplemental Material [55]), which ensures sufficient flexibility for different applications. Remarkably, the PDFs of the Hurst exponent extracted from soft matter [42] and biological [47] experimental data were previously fitted with the bell-shaped unimodal beta distribution with $\lambda_{12}\tau, \lambda_{21}\tau > 1$ [74]. In what follows we basically restrict ourselves to such a shape, however for the sake of comparison we also study the bimodal case corresponding to $\lambda_{12}\tau, \lambda_{21}\tau < 1$. Notably, a bimodal distribution of the Hurst exponents were reported in biological SPT experiments [48]. The mean of $\mathcal{H}(t)$ is given by

$$\langle \mathcal{H}(t)\rangle = \frac{H_1\lambda_{21} + H_2\lambda_{12}}{2\lambda}, \quad (7)$$

while the ACVF is a combination of exponentials (see, e.g., [73] and Sec. III in Supplemental Material [55]),

$$\langle (\mathcal{H}(t) - \langle \mathcal{H}(t)\rangle)(\mathcal{H}(s) - \langle \mathcal{H}(s)\rangle)\rangle = \frac{\lambda_{12}\lambda_{21}(H_2 - H_1)^2}{4\lambda^2(4\lambda^2\tau^2 - 1)} \left(2\lambda\tau e^{-|t-s|/\tau} - e^{-2\lambda|t-s|}\right). \quad (8)$$

We note that other choices of $\mathcal{H}(t)$, for instance the Ornstein-Uhlenbeck process or the squared Ornstein-Uhlenbeck process, also result in an exponentiallike decay of the ACVF (see Sec. IX in Supplemental Material [55]). However, unlike the smoothed telegraph process, for those choices *ad hoc* boundary conditions need to be specified so that $\mathcal{H}$ remains bounded. Moreover, our choice is physically motivated due to the resultant stationary beta distribution of $\mathcal{H}$ and its flexibility to account for both uni- and bimodal distributions.

In Fig. 1(a) we show exemplary trajectories of $\mathcal{H}(t)$, while in Fig. 1(b) we demonstrate the corresponding TeMBM trajectories. In addition, we present sample trajectories of FBM with three different Hurst exponents.

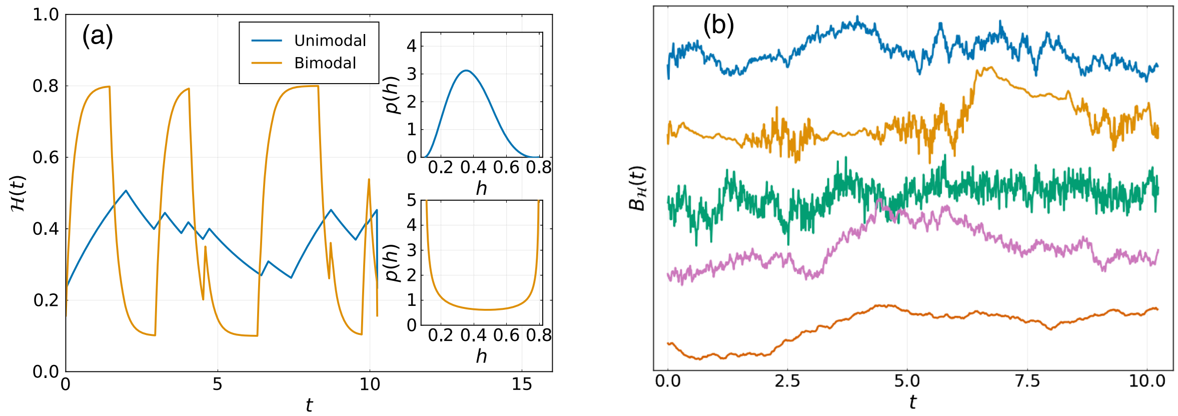

FIG. 1. (a) Single trajectories of $\mathcal{H}(t)$ with the following parameters: $\lambda_{12} = 1$, $\lambda_{21} = 1.5$, $\tau = 3$ (unimodal), $\tau = \frac{1}{4}$ (bimodal), and the levels $H_1 = 0.1$, $H_2 = 0.8$. Insets: the corresponding PDFs given by Eq. (6). (b) Single trajectories corresponding to (from top to bottom) TeMBM (unimodal case), TeMBM (bimodal case), FBM with $H = 0.1$, FBM with $H = 0.4$, and FBM with $H = 0.8$. The individual trajectories are shifted with respect to each other for better visibility.

The simulation algorithms to generate the trajectories of $\mathcal{H}(t)$ and $B_{\mathcal{H}}(t)$ are presented in Sec. IV in Supplemental Material [55]. The intermittent behavior of the trajectory $B_{\mathcal{H}}(t)$ in the bimodal case is contrasted with that of the unimodal case. Indeed, it might be difficult to visually distinguish TeMBM in the unimodal case from FBM [see, e.g., the blue curve vs the pink curve in Fig. 1(b)].

FBM with random Hurst exponent (FBMRE) is a special case of MBM such that $\mathcal{H}(t)$ is constant for each trajectory but changes randomly from trajectory to trajectory. Such an approach is in the spirit of superstatistics [75,76]. The properties of FBMRE with a beta distribution of the Hurst exponent were investigated in [74]. Apparently, the PDF and MSD of such FBMRE and TeMBM are the same for stationary $\mathcal{H}(t)$.

While analyzing stochastic time series, how can one distinguish TeMBM from the hierarchically lower level processes, namely, FBM and FBMRE, all of which exhibit power-law correlations? Before addressing this issue we suggest a method that allows the estimation of the random Hurst exponent from the time averaged mean squared displacement (TAMSD). We recall, for a time series $X = \{X_1, X_2, \ldots, X_N\}$, where $X_i = X(t_i)$ are the observations recorded at time t_i, the TAMSD is defined as

$$\overline{\delta^2(\Delta)} = \frac{1}{N-\Delta}\sum_{j=1}^{N-\Delta}(X_{j+\Delta} - X_j)^2, \qquad (9)$$

where Δ is the lag time. This widely used observable is routinely measured, e.g., in SPT experiments [12]. In the case of FBM and FBMRE the TAMSD behaves as $\overline{\delta^2(\Delta)} \propto \Delta^{2H}$ [77,78], where H is the Hurst exponent of the trajectory for which the TAMSD is computed. Therefore, H can be estimated as the slope of the log-log plot of TAMSD vs lag time. By segmenting a trajectory into multiple segments with overlapping length, we extend this procedure also to obtain estimates of the Hurst exponent that changes along the trajectory (see Sec. V in Supplemental Material [55]). Figure 2 validates this

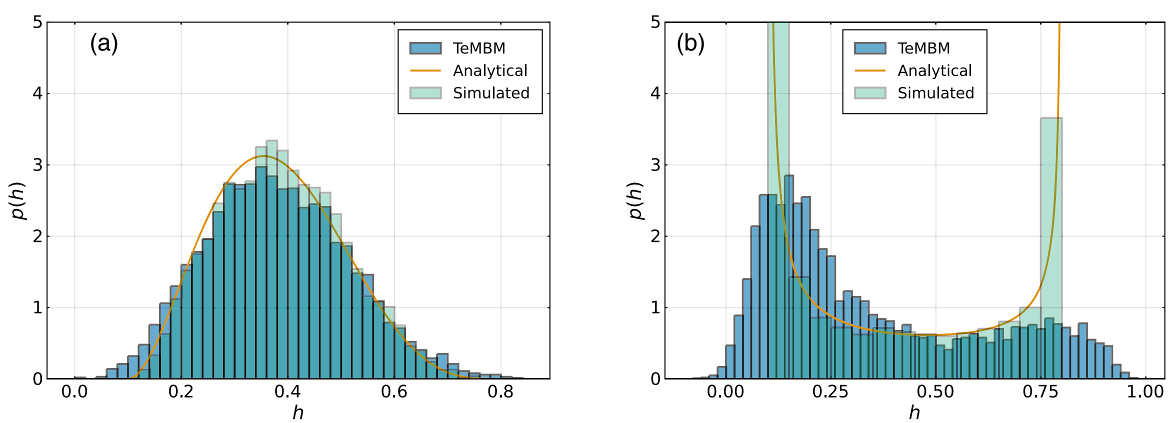

FIG. 2. PDFs of estimated values of the Hurst exponent for (a) unimodal case, (b) bimodal case. The parameters are the same as used in Fig. 1. See text for details.

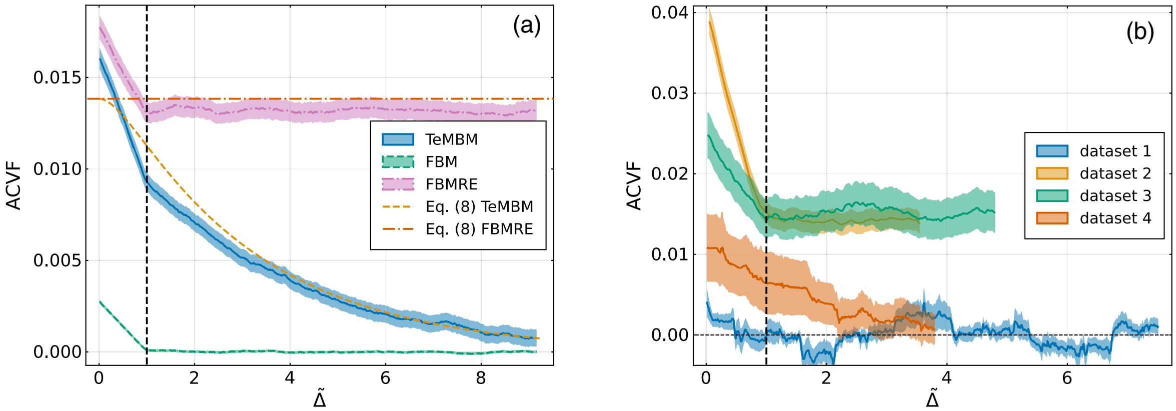

FIG. 3. (a) Sample ACVFs as function of the rescaled lag time $\tilde{\Delta}$ for the estimated Hurst exponent from 5,000 trajectories of TeMBM (unimodal case), FBMRE (unimodal case) and FBM with $H = 0.1$. The parameters of the processes are the same as used in Fig. 1 (see the figure caption for more details). Note that the analytical expression of ACVF for TeMBM is given by Eq. (8) which, upon setting $t = s$, also gives the analytical expression of ACVF for FBMRE with beta-distributed H. (b) Results of the process-distinguishing procedure for real data sets. The shaded regions in both (a) and (b) correspond to 95% confidence intervals. See text for a description of the datasets.

approach. More precisely, it shows that for both the unimodal [Fig. 2(a)] and bimodal [Fig. 2(b)] cases the distribution of estimated Hurst exponents from simulated TeMBM trajectories ("TeMBM") agrees well with the distribution ("Simulated") of the ground truth values of Hurst exponents which generated the simulated trajectories, and also agrees with the analytical stationary distribution ("Analytical").

To distinguish the processes we analyze the sample ACVF (calculated for sample trajectories) of the estimated Hurst exponents (see Sec. VI in Supplemental Material [55]). For FBM, the Hurst exponent is a constant value for each time point, resulting in a zero ACVF of the Hurst exponent. In the case of FBMRE, for each trajectory the Hurst exponent takes on a random value, thereby resulting in a constant, nonzero ACVF equal to the variance of $\mathcal{H}$. Finally, for TeMBM, the Hurst exponent is the smoothed telegraph process and the corresponding ACVF is given by a decaying function [see Eq. (8)]. Importantly, this classification procedure is applicable for discerning any MBM process from FBMRE and FBM.

Figure 3(a) demonstrates the utility of this scheme for simulated TeMBM (unimodal case), FBMRE (unimodal case), and FBM trajectories. The parameters are the same as in Fig. 1. The dashed black vertical line at $\tilde{\Delta} = 1$ depicts the value of the lag time Δ normalized by the segment length used in the algorithm (see Sec. VI in Supplemental Material [55]). We note that although segmentation is not required to estimate the Hurst exponent from FBM and FBMRE trajectories, in our analysis we follow the same procedure for all trajectories without *a priori* assuming the underlying model. Indeed, as expected, the ACVF of the estimated Hurst exponents saturates at the zero level for FBM, saturates at a constant, nonzero value for FBMRE, while it decays exponentially in the case of TeMBM for the chosen values of the parameters. Although the TAMSD-based method slightly underestimates the ACVF of H for FBMRE and TeMBM, Fig. 3(a) shows that the simulation results are very close to the analytical expressions.

In Fig. 3(b) we present the results of the classification procedure applied to different experimental datasets. Dataset 1 consists of the time series of the cumulative sum of temperature anomalies obtained from mean daily temperature data, in the period from 1955-01-01 to 2020-12-31, collected at 10 different meteorological stations in Germany [79,80]. Temperature anomalies are the deviations of the daily temperature at a given calendar day of the year from the average daily temperature at that particular calendar day, where the average is over all years considered, i.e., from 1955 to 2020 [81]. Dataset 2 are trajectories of quantum dots tracked in the cytoplasm of mammalian cells [47] and dataset 3 consists of trajectories of micron-sized beads tracked in mucin hydrogels at acidic conditions ($pH = 2$) and with zero salt concentration [42]. Dataset 4 corresponds to the day-ahead electricity price in the year 2022 from the bidding zone between Germany and Luxembourg [82]. "Bidding zone" here refers to the largest area or region within which electricity producers and consumers submit their bids and offers without any technical constraints. We refer to Sec. VII in Supplemental Material [55] for details on these datasets, and particularly how ensembles of trajectories are created in case of dataset 1 and dataset 4. Figure 3(b) shows that for dataset 1 the sample ACVF of the estimated Hurst exponents is around zero, which we also observe for FBM trajectories in Fig. 3(a). This FBM-like behavior is consistent with previous analyses of such daily temperature data [17,83]. For dataset 2 and dataset 3 one can see that the sample ACVFs for the estimated Hurst exponents stabilize at some nonzero levels, which indicates the correspondence of these datasets to the FBMRE case. This is consistent with the results presented in [74], where we identified beta distributions for the estimated Hurst exponents. For the electricity prices in dataset 4, we clearly see the decay of the sample ACVF of the estimated Hurst exponents, which indicates the multifractional case. In Fig. 3(b) we present the sample ACVF with the first observation on Wednesday. In Fig. 2 in Supplemental Material [55] we show similar results for other starting points which highlights the robustness of the results with regard to the choice of the starting point.

One may ask why it is necessary to distinguish between the three classes of processes. With regards to SPT experiments, FBM with fixed Hurst exponent describes the dynamics of identical particles in homogeneous, viscoelastic media. FBMRE corresponds either to the dynamics of a heterogeneous ensemble of non-identical particles [44,46] or the dynamics in a heterogeneous medium when each particle moves in a domain characterized by its own microstructure properties [41,84,85]. However, the most general cases, which can be mimicked by TeMBM, correspond to media or particle properties that vary in time, or to the situation when a tracked particle explores a large spatial domain characterized by different Hurst exponents. TeMBM is sufficiently generic to describe the case of stochastically varying Hurst exponents while resulting in the observed beta distribution. For experiments with identical particles, distinguishing between FBMRE and TeMBM allows us to separate fluctuations of the environment in time and in space.

As for financial applications, estimates of the Hurst exponent often strongly suggest that a single parameter representing the long-term dependence is insufficient to capture the intricacies of the price evolution. The considerable variation in estimates can be succinctly explained by assuming that the degree of correlations undergoes fluctuations over time [35,86]. This contradicts the *efficient market hypothesis* (EMH) which, within the paradigm of an ordinary Brownian setting, dictates that market prices incorporate all available information instantaneously [87,88]. Indeed, as a consequence, this has led to the development of qualitative models such as *behavioral finance* [89,90], which is based on the study of psychological influence on the behavior of market practitioners, or *adaptive market hypothesis* [91], which relies on the concepts of evolutionary biology. Our proposed model could serve as a quantitative tool complementary to the qualitative models. It could allow the analytical assessment of how much the market prices deviate from EMH at any given time. Fluctuations of $\mathcal{H}(t)$ at the same time could describe the different market consequences and the investors' beliefs [35]. Indeed $\mathcal{H}(t)$ can be understood as the weight assigned at a given time t by an investor to past prices: $\mathcal{H}(t) = 1/2$ indicates an efficient market, $\mathcal{H}(t) > 1/2$ is indicative of a market whose future prices strongly depend on past prices and reacts slowly to new information (*underreaction*), while $\mathcal{H}(t) < 1/2$ denotes the belief that future prices will contradict the current prices and the market reacts strongly to new information (*overreaction*) [35].

Going back to physical systems, we note that TeMBM cannot account for all possible physical mechanisms and manifestations of heterogeneity. Our assumption that $\mathcal{H}(t)$ is a stationary process independent of $B(t)$ ensures that the resultant TeMBM is self-similar (see Theorem 4.1 in [30]), but restricts its applicability to model aging dynamics [92,93]. It is nevertheless an important step in the direction of research focused on the comprehension and implications of heterogeneity in SPT experiments which started with the seminal articles on Brownian yet non-Gaussian diffusion [94,95] and the subsequent development of models with diffusing diffusivity [96–108]. More advanced models should combine stochastic diffusivity with stochastic Hurst exponent. Moreover, while in this Letter we consider a class of self-similar, power-law correlated processes, in light of the apparent heterogeneity in a wide variety of systems exhibiting anomalous diffusion, there is a need to generalize relevant anomalous diffusion models to include stochastic parameters [109,110]. When establishing such generalizations, some care needs to be taken how the time dependence of the Hurst exponent and the diffusivity are incorporated, as shown for FBM-type processes with deterministic protocols [47,111–113]. Concurrently, advanced data analysis methods such as those based on Bayesian statistics [114–116] or machine learning [117–119] need to be developed to identify the best model given some empirical data.

To summarize, we propose a generic, relatively simple analytical model of the multifractional process, namely telegraphic multifractional Brownian motion, that describes the temporal fluctuations of the system during its evolution. The Hurst exponent of this motion undergoes the smoothed telegraph process whose stationary PDF is given by the beta distribution. Such a choice is in agreement with Hurst exponent PDFs obtained in bio- and soft-matter experiments. We provide a methodology to distinguish between three classes of power-law correlated random processes, namely FBM (with fixed Hurst exponent), FBM with Hurst exponent varying between different realizations, and telegraphic multifractional Brownian motion. The examples of the processes taken from biology, climate, and finance illustrate the effectiveness of our approach.

Acknowledgments—We thank Diego Krapf and Matthias Weiss for the dataset of quantum dots tracked in the cytoplasm of mammalian cells (dataset 2), and Caroline E. Wagner for the dataset of beads tracked in mucin hydrogels (dataset 3). The work of A. W. was supported by the National Science Centre, Poland, project 2020/37/B/HS4/00120. R. M. acknowledges funding from the German Science Foundation (DFG grant ME 1535/22-1) and the German Ministry for Education and Research (NSF-BMBF project STAXS). A. C. acknowledges funding from BMBF project 01DK24006 PLASMA-SPIN-ENERGY.

[1] U. Frisch, *Turbulence: The Legacy of A.N. Kolmogorov* (Cambridge University Press, Cambridge, England, 1995), 10.1017/cbo9781139170666.

[2] A. N. Kolmogorov, Curves in a Hilbert space invariant with respect to a one-parameter group of motions, C. R. (Doklady) Acad. Sci. URSS (NS) **26**, 6 (1940).

[3] A. N. Kolmogorov, Wienersche Spiralen und einige andere interessante Kurven im Hilbertschen Raum, C. R. (Doklady) Acad. Sci. URSS (NS) **26**, 115 (1940).

[4] A. M. Yaglom and M. S. Pinsker, Random processes with stationary increments of order n, Dokl. Acad. Nauk USSR **90**, 731 (1953).

[5] A. M. Yaglom, Correlation theory of processes with random stationary n^{th} increments, Mat. Sb. **79**, 141 (1955).

[6] A. M. Yaglom, *Correlation Theory of Stationary and Related Random Functions: Supplementary Notes and References* (Springer Science & Business Media, New York, 2012).

[7] B. B. Mandelbrot and J. W. V. Ness, Fractional Brownian motions, fractional noises and applications, SIAM Rev. **10**, 422 (1968).

[8] Y. Mishura, *Stochastic Calculus for Fractional Brownian Motion and Related Processes* (Springer, New York, 2008).

[9] M. M. Meerschaert and A. Sikorskii, *Stochastic Models for Fractional Calculus* (Walter de Gruyter GmbH & Co KG, Berlin, 2019), Vol. 43.

[10] I. M. Sokolov, Models of anomalous diffusion in crowded environments, Soft Matter **8**, 9043 (2012).

[11] F. Höfling and T. Franosch, Anomalous transport in the crowded world of biological cells, Rep. Prog. Phys. **76**, 046602 (2013).

[12] R. Metzler, J. H. Jeon, A. G. Cherstvy, and E. Barkai, Anomalous diffusion models and their properties: Non-stationarity, non-ergodicity, and ageing at the centenary of single particle tracking, Phys. Chem. Chem. Phys. **16**, 24128 (2014).

[13] P. Doukhan, *Stochastic Models for Time Series* (Springer, New York, 2018).

[14] Z. Struzik, M. Dekking, J. Lévy-Véhel, E. Lutton, and C. Tricot, Fractals: Theory and application in engineering, in *Chap. Local Effective Hölder Exponent Estimation on the Wavelet Transform Maxima Tree* (Springer Verlag, Berlin, 1999), pp. 93–112.

[15] R. Jennane, W. J. Ohley, S. Majumdar, and G. Lemineur, Fractal analysis of bone x-ray tomographic microscopy projections, IEEE Trans. Med. Imaging **20**, 443 (2001).

[16] M.-A. Miville-Deschênes, F. Levrier, and E. Falgarone, On the use of fractional Brownian motion simulations to determine the three-dimensional statistical properties of interstellar gas, Astrophys. J. **593**, 831 (2003).

[17] S. Thapa, A. Wyłomańska, G. Sikora, C. E. Wagner, D. Krapf, H. Kantz, A. V. Chechkin, and R. Metzler, Leveraging large-deviation statistics to decipher the stochastic properties of measured trajectories, New J. Phys. **23**, 013008 (2021).

[18] I. M. Jánosi, A. Padash, J. A. C. Gallas, and H. Kantz, Passive tracer advection in the equatorial pacific region: Statistics, correlations and a model of fractional Brownian motion, Ocean Sci. **18**, 307 (2022).

[19] G. Korvin, *Fractal Models in the Earth Sciences* (Elsevier, New York, 1992).

[20] O. Vilk, E. Aghion, R. Nathan, S. Toledo, R. Metzler, and M. Assaf, Classification of anomalous diffusion in animal movement data using power spectral analysis, J. Phys. A **55**, 334004 (2022).

[21] O. Vilk, E. Aghion, T. Avgar, C. Beta, O. Nagel, A. Sabri, R. Sarfati, D. K. Schwartz, M. Weiss, D. Krapf *et al.*, Unravelling the origins of anomalous diffusion: From molecules to migrating storks, Phys. Rev. Res. **4**, 033055 (2022).

[22] D. Ernst, M. Hellmann, J. Köhler, and M. Weiss, Fractional Brownian motion in crowded fluids, Soft Matter **8**, 4886 (2012).

[23] D. Krapf, N. Lukat, E. Marinari, R. Metzler, G. Oshanin, C. Selhuber-Unkel, A. Squarcini, L. Stadler, M. Weiss, and X. Xu, Spectral content of a single non-Brownian trajectory, Phys. Rev. X **9**, 011019 (2019).

[24] S. Janušonis, N. Detering, R. Metzler, and T. Vojta, Serotonergic axons as fractional Brownian motion paths: Insights into the self-organization of regional densities, Front. Comput. Neurosci. **14**, 56 (2020).

[25] J. Gatheral, T. Jaisson, and M. Rosenbaum, Volatility is rough, in *Commodities* (Chapman and Hall/CRC, London, 2022), pp. 659–690.

[26] J. Lévy-Véhel and R. Peltier, Multifractional Brownian motion: Definition and preliminary results, Rapport de recherche de l'INRIA **2645** (1995).

[27] A. Benassi, S. Jaffard, and D. Roux, Elliptic Gaussian random processes, Rev. Math. Iberoam. **13**, 19 (1997).

[28] S. Cohen, From self-similarity to local self-similarity: The estimation problem, in *Fractals: Theory and Applications in Engineering* (Springer, New York, 1999), pp. 3–16.

[29] A. Ayache, S. Cohen, and J. L. Véhel, The covariance structure of multifractional Brownian motion, with application to long range dependence, in *2000 IEEE International Conference on Acoustics, Speech, and Signal Processing. Proceedings (Cat. No. 00CH37100)* (IEEE, New York, 2000), Vol. 6, pp. 3810–3813.

[30] A. Ayache and M. S. Taqqu, Multifractional processes with random exponent, Publicacions Matemàtiques **49**, 459 (2005).

[31] S. A. Stoev and M. S. Taqqu, How rich is the class of multifractional Brownian motions?, Stoch. Proc. Appl. **116**, 200 (2006).

[32] J. Ryvkina, Fractional Brownian Motion with variable Hurst parameter: Definition and properties, J. Theor. Probab. **28**, 866 (2015).

[33] A. Ayache and P. R. Bertrand, A process very similar to multifractional Brownian motion, in *Recent Developments*

in Fractals and Related Fields (Springer, New York, 2010), pp. 311–326.

[34] S. Bianchi, A. Pantanella, and A. Pianese, Modeling stock prices by multifractional Brownian motion: An improved estimation of the pointwise regularity, Quant. Finance **13**, 1317 (2013).

[35] S. Bianchi and A. Pianese, Multifractional processes in finance, Risk Decis. Anal. **5**, 1 (2014).

[36] C. S. Tapiero, O. J. Tapiero, and G. Jumarie, The price of granularity and fractional finance, Risk Decis. Anal. **5**, 7 (2016).

[37] S. Combrexelle, H. Wendt, N. Dobigeon, J.-Y. Tourneret, S. McLaughlin, and P. Abry, Bayesian estimation of the multifractality parameter for image texture using a whittle approximation, IEEE Trans. Image Process. **24**, 2540 (2015).

[38] A. Mastalerz-Kodzis, Application of the multifractional Brownian motion process in spatial analyses, Argumenta Oeconomica Cracoviensia **18**, 83 (2018).

[39] N. Pawar, C. Donth, and M. Weiss, Anisotropic diffusion of macromolecules in the contiguous nucleocytoplasmic fluid during eukaryotic cell division, Curr. Biol. **24**, 1905 (2014).

[40] N. Schweizer, N. Pawar, M. Weiss, and H. Maiato, An organelle-exclusion envelope assists mitosis and underlies distinct molecular crowding in the spindle region, J. Cell Biol. **210**, 695 (2015).

[41] O. Stiehl and M. Weiss, Heterogeneity of crowded cellular fluids on the meso-and nanoscale, Soft Matter **12**, 9413 (2016).

[42] C. E. Wagner, B. S. Turner, M. Rubinstein, G. H. McKinley, and K. Ribbeck, A rheological study of the association and dynamics of MUC5ac gels, Biomacromolecules **18**, 3654 (2017).

[43] A. A. Sadoon and Y. Wang, Anomalous, non-Gaussian, viscoelastic, and age-dependent dynamics of histonelike nucleoid-structuring proteins in live Escherichia coli, Phys. Rev. E **98**, 042411 (2018).

[44] A. G. Cherstvy, O. Nagel, C. Beta, and R. Metzler, Non-Gaussianity, population heterogeneity, and transient superdiffusion in the spreading dynamics of amoeboid cells, Phys. Chem. Chem. Phys. **20**, 23034 (2018).

[45] A. G. Cherstvy, S. Thapa, C. E. Wagner, and R. Metzler, Non-Gaussian, non-ergodic, and non-Fickian diffusion of tracers in mucin hydrogels, Soft Matter **15**, 2526 (2019).

[46] S. Thapa, N. Lukat, C. Selhuber-Unkel, A. G. Cherstvy, and R. Metzler, Transient superdiffusion of polydisperse vacuoles in highly motile amoeboid cells, J. Chem. Phys. **150** 144901 (2019).

[47] A. Sabri, X. Xu, D. Krapf, and M. Weiss, Elucidating the origin of heterogeneous anomalous diffusion in the cytoplasm of mammalian cells, Phys. Rev. Lett. **125**, 058101 (2020).

[48] D. Han, N. Korabel, R. Chen, M. Johnston, A. Gavrilova, V. J. Allan, S. Fedotov, and T. A. Waigh, Deciphering anomalous heterogeneous intracellular transport with neural networks, eLife **9**, e52224 (2020).

[49] R. Benelli and M. Weiss, From sub- to superdiffusion: Fractional Brownian motion of membraneless organelles in early C. elegans embryos, New J. Phys. **23**, 063072 (2021).

[50] K. Speckner and M. Weiss, Single-particle tracking reveals anti-persistent subdiffusion in cell extracts, Entropy **23**, 892 (2021).

[51] J. Janczura, M. Balcerek, K. Burnecki, A. Sabri, M. Weiss, and D. Krapf, Identifying heterogeneous diffusion states in the cytoplasm by a hidden Markov model, New J. Phys. **23**, 053018 (2021).

[52] H. T. Perkins, V. J. Allan, and T. A. Waigh, Network organisation and the dynamics of tubules in the endoplasmic reticulum, Sci. Rep. **11**, 16230 (2021).

[53] N. Korabel, D. Han, A. Taloni, G. Pagnini, S. Fedotov, V. Allan, and T. A. Waigh, Local analysis of heterogeneous intracellular transport: Slow and fast moving endosomes, Entropy **23**, 958 (2021).

[54] T. A. Waigh and N. Korabel, Heterogeneous anomalous transport in cellular and molecular biology, Rep. Prog. Phys. **86**, 126601 (2023).

[55] See Supplemental Material at http://link.aps.org/supplemental/10.1103/PhysRevLett.134.197101, which includes Refs. [56–61], for additional information about the analytical calculations, numerical simulations, and the analyzed datasets.

[56] J. M. Sancho, Stochastic processes driven by dichotomous Markov noise: Some exact dynamical results, J. Math. Phys. (N.Y.) **25**, 354 (1984).

[57] V. E. Shapiro and V. M. Loginov, "Formulae of differentiation" and their use for solving stochastic equations, Physica (Amsterdam) **91A**, 563 (1978).

[58] A. V. Skorokhod, Stochastic equations for diffusion processes in a bounded region, Theory Probab. Its Appl. **6**, 264 (1961).

[59] V. Giorno, A. G. Nobile, and L. Ricciardi, On some diffusion approximations to queueing systems, Adv. Appl. Probab. **18**, 991 (1986).

[60] A. R. Ward and P. W. Glynn, A diffusion approximation for a Markovian queue with reneging, Queueing Syst. Theory Appl. **43**, 103 (2003).

[61] M. Balcerek, Python notebook including the simulation and estimation codes, https://github.com/MichalBalcerek/Multifractional-Brownian-motion-with-telegraphic-stochastically-varying-exponent (2024).

[62] S. T. Eada, V. Pozdnyakov, and J. Yan, Discretely observed Brownian motion governed by telegraph signal process: Estimation and application to finance, Stat. Inference Stoch. Process. **28**, 1 (2025).

[63] N. Ratanov, Telegraph processes with random jumps and complete market models, Methodol. Comput. Appl. Probab. **17**, 677 (2015).

[64] O. López and N. Ratanov, Option pricing driven by a telegraph process with random jumps, J. Appl. Probab. **49**, 838 (2012).

[65] A. D. Kolesnik and N. Ratanov, *Telegraph Processes and Option Pricing* (Springer Series in Statistics, New York, 2013).

[66] J. Paulsson, Models of stochastic gene expression, Phys. Life Rev. **2**, 157 (2005).

[67] L. S. Tsimring, Noise in biology, Rep. Prog. Phys. **77**, 026601 (2014).

[68] D. Mizuno, C. Tardin, C. F. Schmidt, and F. C. MacKintosh, Nonequilibrium mechanics of active cytoskeletal networks, Science **315**, 370 (2007).

[69] F. C. MacKintosh and A. J. Levine, Nonequilibrium mechanics and dynamics of motor-activated gels, Phys. Rev. Lett. **100**, 018104 (2008).

[70] C. P. Brangwynne, G. H. Koenderink, F. C. MacKintosh, and D. A. Weitz, Nonequilibrium microtubule fluctuations in a model cytoskeleton, Phys. Rev. Lett. **100**, 118104 (2008).

[71] M. Guo, A. J. Ehrlicher, M. H. Jensen, M. Renz, J. R. Moore, R. D. Goldman, J. Lippincott-Schwartz, F. C. Mackintosh, and D. A. Weitz, Probing the stochastic, motor-driven properties of the cytoplasm using force spectrum microscopy, Cell **158**, 822 (2014).

[72] G. Gradziuk, G. Torregrosa, and C. P. Broedersz, Irreversibility in linear systems with colored noise, Phys. Rev. E **105**, 024118 (2022).

[73] R. FitzHugh, Statistical properties of the asymmetric random telegraph signal, with applications to single-channel analysis, Math. Biosci. **64**, 75 (1983).

[74] M. Balcerek, K. Burnecki, S. Thapa, A. Wyłomańska, and A. Chechkin, Fractional Brownian motion with random Hurst exponent: Accelerating diffusion and persistence transitions, Chaos **32**, 093114 (2022).

[75] C. Beck, Dynamical foundations of nonextensive statistical mechanics, Phys. Rev. Lett. **87**, 180601 (2001).

[76] C. Beck and E. G. Cohen, Superstatistics, Physica (Amsterdam) **322A**, 267 (2003).

[77] W. Deng and E. Barkai, Ergodic properties of fractional Brownian-Langevin motion, Phys. Rev. E **79**, 011112 (2009).

[78] H. Woszczek, A. Wylomanska, and A. Chechkin, Riemann-Liouville fractional Brownian motion with random Hurst exponent, Chaos **35**, 023145 (2025).

[79] A. M. G. K. Tank *et al.*, Daily dataset of 20th-century surface air temperature and precipitation series for the European climate assessment, International Journal of Climatology **22**, 1441 (2002).

[80] European climate assessment & dataset project webpage, http://www.ecad.eu (2024).

[81] J. M. Wallace and P. V. Hobbs, *Atmospheric Science: An Introductory Survey* (Elsevier, New York, 2006), Vol. 92.

[82] ENTSO-E webpage, entsoe.eu (2024).

[83] M. Massah and H. Kantz, Confidence intervals for time averages in the presence of long-range correlations, a case study on earth surface temperature anomalies, Geophys. Res. Lett. **43**, 9243 (2016).

[84] I. Y. Wong, M. L. Gardel, D. R. Reichman, E. R. Weeks, M. T. Valentine, A. R. Bausch, and D. A. Weitz, Anomalous diffusion probes microstructure dynamics of entangled F-actin networks, Phys. Rev. Lett. **92**, 178101 (2004).

[85] M. Levin, G. Bel, and Y. Roichman, Measurements and characterization of the dynamics of tracer particles in an actin network, J. Chem. Phys. **154**, 144901 (2021).

[86] S. Bianchi and A. Pianese, Multifractional properties of stock indices decomposed by filtering their pointwise Hölder regularity, Int. J. Theor. Appl. Finance **11**, 567 (2008).

[87] E. F. Fama, Efficient capital markets, J. Finance **25**, 383 (1970).

[88] B. G. Malkiel, The efficient market hypothesis and its critics, J. Econ. Perspect. **17**, 59 (2003).

[89] C. Camerer, S. Issacharoff, G. Loewenstein, T. O'Donoghue, and M. Rabin, Regulation for conservatives: Behavioral economics and the case for “asymmetric paternalism,” Univ. Pennsylvania Law Rev. **151**, 1211 (2003).

[90] G. Muradoglu and N. Harvey, Behavioural finance: The role of psychological factors in financial decisions, Rev. Behav. Finance **4**, 68 (2012).

[91] A. W. Lo, The adaptive markets hypothesis: Market efficiency from an evolutionary perspective, J. Portfolio Manage. **30**, 15 (2004).

[92] A. V. Weigel, B. Simon, M. M. Tamkun, and D. Krapf, Ergodic and nonergodic processes coexist in the plasma membrane as observed by single-molecule tracking, Proc. Natl. Acad. Sci. U.S.A. **108**, 6438 (2011).

[93] S. A. Tabei, S. Burov, H. Y. Kim, A. Kuznetsov, T. Huynh, J. Jureller, L. H. Philipson, A. R. Dinner, and N. F. Scherer, Intracellular transport of insulin granules is a subordinated random walk, Proc. Natl. Acad. Sci. U.S.A. **110**, 4911 (2013).

[94] B. Wang, S. M. Anthony, S. C. Bae, and S. Granick, Anomalous yet Brownian, Proc. Natl. Acad. Sci. U.S.A. **106**, 15160 (2009).

[95] B. Wang, J. Kuo, S. C. Bae, and S. Granick, When Brownian diffusion is not Gaussian, Nat. Mater. **11**, 481 (2012).

[96] M. V. Chubynsky and G. W. Slater, Diffusing diffusivity: A model for anomalous, yet Brownian, diffusion, Phys. Rev. Lett. **113**, 098302 (2014).

[97] R. Jain and K. L. Sebastian, Diffusion in a crowded, rearranging environment, J. Phys. Chem. B **120**, 3988 (2016).

[98] A. V. Chechkin, F. Seno, R. Metzler, and I. M. Sokolov, Brownian yet non-Gaussian diffusion: From superstatistics to subordination of diffusing diffusivities, Phys. Rev. X **7**, 021002 (2017).

[99] N. Tyagi and B. J. Cherayil, Non-Gaussian Brownian diffusion in dynamically disordered thermal environments, J. Phys. Chem. B **121**, 7204 (2017).

[100] Y. Lanoiselée, N. Moutal, and D. S. Grebenkov, Diffusion-limited reactions in dynamic heterogeneous media, Nat. Commun. **9**, 4398 (2018).

[101] V. Sposini, A. V. Chechkin, F. Seno, G. Pagnini, and R. Metzler, Random diffusivity from stochastic equations: Comparison of two models for Brownian yet non-Gaussian diffusion, New J. Phys. **20**, 043044 (2018).

[102] W. Wang, A. G. Cherstvy, A. V. Chechkin, S. Thapa, F. Seno, X. Liu, and R. Metzler, Fractional Brownian motion with random diffusivity: Emerging residual nonergodicity below the correlation time, J. Phys. A **53**, 474001 (2020).

[103] W. Wang, F. Seno, I. M. Sokolov, A. V. Chechkin, and R. Metzler, Unexpected crossovers in correlated random-diffusivity processes, New J. Phys. **22**, 083041 (2020).

[104] E. Barkai and S. Burov, Packets of diffusing particles exhibit universal exponential tails, Phys. Rev. Lett. **124**, 060603 (2020).

[105] R. Pastore, A. Ciarlo, G. Pesce, F. Greco, and A. Sasso, Rapid Fickian yet non-Gaussian diffusion after subdiffusion, Phys. Rev. Lett. **126**, 158003 (2021).
[106] J. M. Miotto, S. Pigolotti, A. V. Chechkin, and S. Roldán-Vargas, Length scales in Brownian yet non-Gaussian dynamics, Phys. Rev. X **11**, 031002 (2021).
[107] F. Rusciano, R. Pastore, and F. Greco, Fickian non-Gaussian diffusion in glass-forming liquids, Phys. Rev. Lett. **128**, 168001 (2022).
[108] R. Großmann, L. S. Bort, T. Moldenhawer, M. Stange, S. S. Panah, R. Metzler, and C. Beta, Non-Gaussian displacements in active transport on a carpet of motile cells, Phys. Rev. Lett. **132**, 088301 (2024).
[109] M. Arutkin and S. Reuveni, Doubly stochastic continuous time random walk, Phys. Rev. Res. **6**, L012033 (2024).
[110] Y. Chen, X. Wang, and M. Ge, Lévy-walk-like Langevin dynamics with random parameters, Chaos **34**, 013109 (2024).
[111] W. Wang, M. Balcerek, K. Burnecki, A. V. Chechkin, S. Janušonis, J. Ślęzak, T. Vojta, A. Wyłomańska, and R. Metzler, Memory-multi-fractional Brownian motion with continuous correlations, Phys. Rev. Res. **5**, L032025 (2023).
[112] J. Ślęzak and R. Metzler, Minimal model of diffusion with time changing Hurst exponent, J. Phys. A **56**, 35LT01 (2023).
[113] M. Balcerek, A. Wyłomańska, K. Burnecki, R. Metzler, and D. Krapf, Modelling intermittent anomalous diffusion with switching fractional Brownian motion, New J. Phys. **25**, 103031 (2023).
[114] J. Krog, L. H. Jacobsen, F. W. Lund, D. Wüstner, and M. A. Lomholt, Bayesian model selection with fractional Brownian motion, J. Stat. Mech. (2018) 093501.
[115] S. Thapa, M. A. Lomholt, J. Krog, A. G. Cherstvy, and R. Metzler, Bayesian analysis of single-particle tracking data using the nested-sampling algorithm: Maximum-likelihood model selection applied to stochastic-diffusivity data, Phys. Chem. Chem. Phys. **20**, 29018 (2018).
[116] S. Thapa, S. Park, Y. Kim, J. H. Jeon, R. Metzler, and M. A. Lomholt, Bayesian inference of scaled versus fractional Brownian motion, J. Phys. A **55**, 194003 (2022).
[117] G. Muñoz-Gil *et al.*, Objective comparison of methods to decode anomalous diffusion, Nat. Commun. **12**, 6253 (2021).
[118] H. Seckler and R. Metzler, Bayesian deep learning for error estimation in the analysis of anomalous diffusion, Nat. Commun. **13**, 6717 (2022).
[119] H. Seckler, J. Szwabinski, and R. Metzler, Machine-learning solutions for the analysis of single-particle diffusion trajectories, J. Phys. Chem. Lett. **14**, 7910 (2023).